

On the nature of spatiotemporal light bullets in bulk Kerr media

D. Majus¹, G. Tamošauskas¹, I. Gražulevičiūtė¹, N. Garejev¹, A. Lotti², A. Couairon³, D. Faccio⁴, A. Dubietis¹

¹*Department of Quantum Electronics, Vilnius University,
Saulėtekio Ave. 9, Building 3, LT-10222 Vilnius, Lithuania*

²*Dipartimento di Scienza e Alta Tecnologia, Università degli Studi dell'Insubria, Via Valleggio 11, I-22100 Como, Italy*

³*Centre de Physique Théorique, CNRS, Ecole Polytechnique, F-91128 Palaiseau, France and*

⁴*School of Engineering & Physical Sciences, Heriot-Watt University, Edinburgh, UK*

(Dated: March 10, 2014)

We present a detailed experimental investigation, which uncovers the nature of light bullets generated from self-focusing in a bulk dielectric medium with Kerr nonlinearity in the anomalous group velocity dispersion regime. By high dynamic range measurements of three-dimensional intensity profiles, we demonstrate that the light bullets consist of a sharply localized high-intensity core, which carries the self-compressed pulse and contains approximately 25% of the total energy, and a ring-shaped spatiotemporal periphery. *Sub-diffractive* propagation along with *dispersive broadening* of the light bullets in free space after they exit the nonlinear medium indicate a strong space-time coupling within the bullet. This finding is confirmed by measurements of spatiotemporal energy density flux that exhibits the same features as stationary, polychromatic Bessel beam, thus highlighting the physical nature of the light bullets.

PACS numbers: 42.65.Jx, 42.65.Tg

Propagation-invariant electromagnetic wave-packets – light bullets, are long sought in many areas of modern optics and attract a great deal of interest in fundamental and applied research [1]. Generation of three-dimensional light bullets, which propagate in the medium without natural dispersive broadening and diffractive spreading, is a non-trivial task from the analytical and numerical points of view, and even more complicated to achieve in real experimental settings [2–4].

The pursuit for three-dimensional light bullets considers two essentially different physical concepts. The first is based on the generation of spatiotemporal solitons, which could be regarded as ideal light bullets with rapidly (exponentially) decaying tails, constituting a high degree of energy localization. Formation of the spatiotemporal soliton relies on simultaneous balancing of diffraction and dispersion by nonlinear effects, such as self-focusing and self-phase modulation [5]. In the first approximation, these conditions could be met in media with Kerr nonlinearity in the anomalous group velocity dispersion (GVD) range [5]. However, the proposed light bullet is a three dimensional extension of the universal Townes profile, therefore possessing similar properties: it forms only at the nonlinear focus [6], and is modulationally unstable [7]. Therefore, for achieving a spatiotemporal invariant propagation, linear and nonlinear optical properties of the medium must be suitably tailored, see e.g. [8–12], thus raising difficult technological challenges. So far, to the best of our knowledge, experimental demonstration of truly three dimensional light bullets was reported only in a two-dimensional array of coupled waveguides featuring quasi-instantaneous cubic nonlinearity and a periodic, transversally modulated refractive index [13].

The second concept for achieving light bullets is based on the precise tailoring of the input wave packet so as

to match the material properties, without the need for optical nonlinearities, i.e. defeating the natural diffractive spreading and dispersive broadening in the linear propagation regime. Linear light bullets are non-solitary, weakly localized wave packets, whose stationary propagation is achieved due to Bessel-like profile of the beam, whose spectral components are distributed over certain propagation cones, so as to continuously refill the axial part, which contains an ultrashort pulse. Moreover, this approach is equally effective in media with normal, as well as anomalous GVD. To this end, non-solitary, weakly localized spatiotemporal linear light bullets have been experimentally demonstrated in the form of the X-waves [14], Airy bullets [15, 16] and ultrashort-pulsed Bessel-like beams [17]. However, practical realizations of the linear light bullets require precise control of propagation angles and phases of the spectral components, and therefore intricate experimental techniques.

A much more straightforward route for achieving non-solitary, weakly localized light bullets is based on self-resaping of the entire wave-packet (ultrashort pulsed laser beam) by means of nonlinear effects, producing the nonlinear analogs of the X-waves [18, 19] and Airy bullets [20]. In particular, spontaneous formation of the nonlinear X-waves was demonstrated by means of femtosecond filamentation in transparent dielectric media, where the input Gaussian-shaped wave packet self-adjusts its spatiotemporal shape via nonlinear effects into a specific spatiotemporal X shape, which maintains its stationarity even in the presence of the nonlinear losses [21–23]. However, pulse splitting which occurs during filamentation of intense femtosecond pulses in the normal GVD regime [24], prevents formation of a single X wave.

Conversely, studies of filamentation in the conditions of anomalous GVD predicted the generation of isolated spa-

tially and temporally compressed pulses [25–30]. Recent investigations have uncovered a filamentation regime, in which quasi-stable three-dimensional non-spreading-pulses are generated [31]. However, there remain relevant unanswered questions regarding the interpretation of these light bullets. In this Letter we explicitly demonstrate that the light bullets generated by self-focusing of femtosecond-pulsed beams in bulk dielectric media with instantaneous Kerr nonlinearity and anomalous group velocity dispersion are polychromatic Bessel-like wave-packets, which bear the basic properties of the nonlinear O-waves [32], as verified by simultaneous measurements of spatiotemporal profiles, frequency-resolved angular spectra, near field intensity distributions, linear and nonlinear propagation features and energy density flux.

The experiment was performed using 90 fs Gaussian pulses with center wavelength of $1.8 \mu\text{m}$ from a commercial, Ti:sapphire laser system-pumped optical parametric amplifier (Topas C, Light Conversion Ltd.). Its output beam (an idler wave, in present case) was suitably attenuated, spatially filtered and focused by an $f = +100 \text{ mm}$ lens into $45\text{-}\mu\text{m}$ (FWHM) spot size which was located on the front face of the nonlinear medium (sapphire sample). The input pulse energy of $3.1 \mu\text{J}$ (corresponding to $3.4 P_{\text{cr}}$, where $P_{\text{cr}} = 10 \text{ MW}$ is the critical power for self-focusing in sapphire) was set so as to induce a light filament, which formed after 4 mm of propagation, as verified by the supercontinuum emission in the visible spectral range. The spatiotemporal intensity distribution at the output of sapphire sample was measured by three-dimensional imaging technique, based on recording spatially-resolved cross-correlation function, see e.g. [33]. More specifically, the output beam was imaged (with $5\times$ magnification) onto a $20\text{-}\mu\text{m}$ -thick beta-barium borate crystal and gated by means of broadband sum-frequency generation with a short, 25-fs pulse with central wavelength of 720 nm from a noncollinear optical parametric amplifier (Topas-White, Light Conversion Ltd.), which was pumped by the second harmonic of Ti:sapphire laser system. The cross-correlation signal with center wavelength of 515 nm was then imaged (with $1.8\times$ magnification) onto the CCD camera (Grasshopper 2, Point Grey) with a pixel size of $4.4 \mu\text{m}$ and 14-bit dynamic range. By changing the time delay of the gating pulse in a 8-fs step, we acquired a sequence of cross-correlation images, which afterwards were merged together to reproduce the entire spatiotemporal intensity distribution of the light bullet.

Evolution of the spatiotemporal intensity distribution over propagation distance z was captured by placing sapphire samples of different lengths in such a way, that the output face of the sample was always kept at the same fixed position, while moving the focusing lens accordingly, to ensure the location of the input focal plane at the front face of the sample. Figure 1 presents the spatiotemporal intensity profiles of the wave-packet as mea-

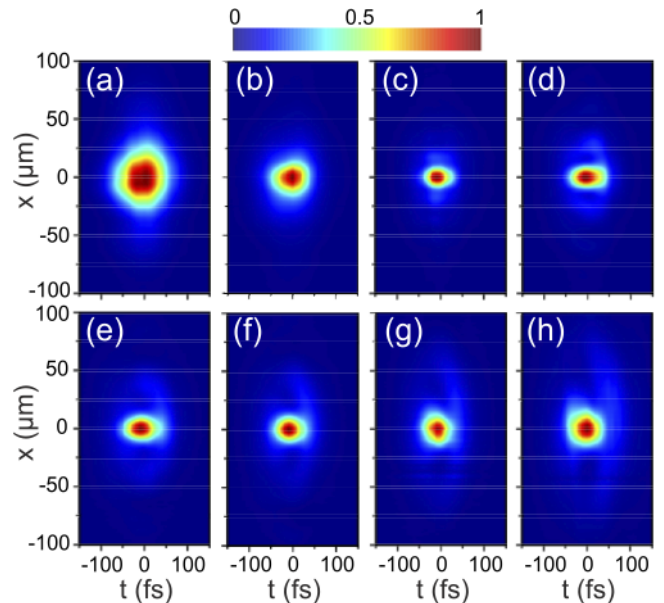


FIG. 1: (Color online) Spatiotemporal intensity distributions of self-focusing Gaussian wave-packet, which transforms into a light bullet, as measured at various propagation lengths z in sapphire: (a) $z = 0 \text{ mm}$, (b) $z = 3.1 \text{ mm}$, (c) $z = 4.2 \text{ mm}$, (d) $z = 6.0 \text{ mm}$, (e) $z = 8.2 \text{ mm}$, (f) $z = 9.0 \text{ mm}$, (g) $z = 12.3 \text{ mm}$, (h) $z = 15.2 \text{ mm}$.

sured at various propagation distances in sapphire, showing how the input Gaussian wave-packet transforms into a spatially and temporally compressed three-dimensional light bullet. Over the first few mm of propagation, the input Gaussian beam shrinks due to self-focusing and the input Gaussian pulse experiences self-compression due to the interplay between self-phase modulation and anomalous GVD. After the nonlinear focus ($z = 4.2 \text{ mm}$), the wave-packet transforms into a spatially and temporally compressed three-dimensional light bullet, which has FWHM diameter of $15 \mu\text{m}$ and pulse duration of 40 fs, as evaluated from the deconvolution of the on-axis cross-correlation function. High dynamic range measurements reveal that the light bullet consists of a sharply localized high-intensity core, which carries the self-compressed pulse and a low-intensity, ring shaped spatiotemporal periphery, and propagates without an apparent change of its spatiotemporal shape. Propagation dynamics of the light bullet are summarized in Fig. 2, where full circles show the beam width and pulse duration versus propagation distance, demonstrating that high intensity core maintains its localization over more than 10 mm of propagation, that exceeds 25 Rayleigh ranges, as calculated for the Gaussian beam of equivalent dimensions.

In a further experiment, where the light bullet after 6 mm of propagation in sapphire was thereafter let to propagate in free space (air), we recorded interesting and very important propagation features. We observe gradual increase of both, spatial and, more importantly, temporal

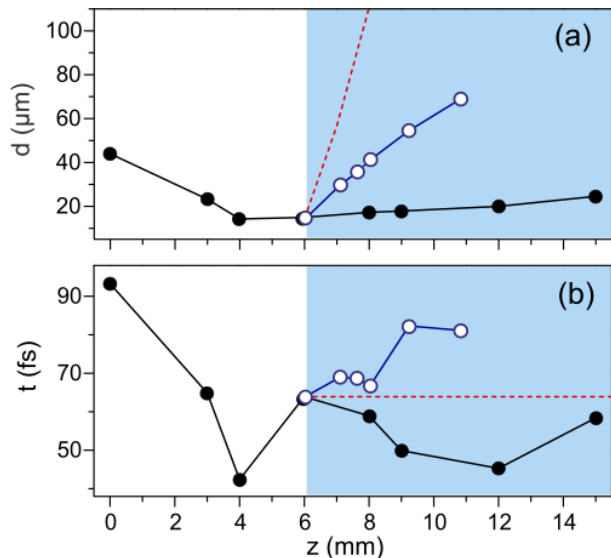


FIG. 2: (Color online) Evolution of (a) beam FWHM diameter and (b) pulsewidth versus propagation distance. Full circles show formation and propagation dynamics of the light bullet in sapphire, as summarized from Fig. 1. Open circles show propagation of the light bullet in free space (air), which starts at $z = 6$ mm. Dashed curves indicate the expected free-space propagation features of a strongly localized Gaussian wave packet.

dimensions of the central core, as the propagation distance in free space increases, as shown by open circles in Fig. 2. These data are compared with the calculated linear evolution of a strongly localized Gaussian wave-packet with identical spatial and temporal dimensions (shown by the dashed curves), which represent the expected spreading of a soliton-like object in free space. The distinctive differences in free space propagation between the present light bullet and a soliton-like object are immediately clear: the diffraction spreading of the bullet is almost 5 times less than that of a Gaussian-shaped beam, and its temporal width increases by a factor of 1.3, just after 3 mm of propagation, in the absence of dispersion, while for a soliton-like object it is expected to remain constant. These results demonstrate that the light bullets, as they exit the nonlinear medium, exhibit *sub-diffractive* and *dispersive* propagation in free space, that is incompatible with the behavior of highly localized spatiotemporal soliton-like objects. The linear and nonlinear propagation features of the light bullets arise from dramatic spatiotemporal reshaping of the input Gaussian wave-packet and resulting strong space-time coupling, which is a distinctive property of conically-shaped wave packets [34].

In the support of this claim, we studied the relevant characteristics of the light bullet in more detail. Figure 3 illustrates the spatial profiles of the input Gaussian beam and the light bullet, as recorded at different propagation distances in sapphire, and obtained by time integration

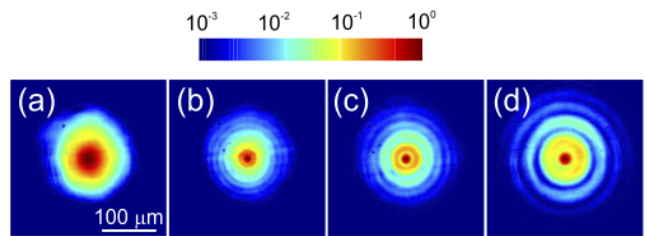


FIG. 3: (Color online) Spatial profiles of (a) the input beam at $z = 0$ mm and the light bullet at (c) $z = 4.2$ mm, (d) $z = 6.0$ mm, (e) $z = 9.0$ mm.

of spatiotemporal profiles presented in Fig. 1. The spatial profiles are presented in logarithmic intensity scale and reveal an intense central core, which contains approximately 25% of the total energy and is surrounded by a low-intensity concentric ring-shaped periphery, thus resembling a distinct Bessel-like intensity distribution, which emerges from the interplay of self-focusing, nonlinear absorption and diffraction [35]. A Bessel-like intensity distribution of the light bullet explains the spatial features of the central core observed in the experiment: its robustness during the nonlinear propagation in sapphire, as well as sub-diffractive propagation in free space, which are achieved via energy refilling from the beam periphery [35, 36].

Figure 4 highlights the characteristic spatiotemporal properties of the input wave packet and the light bullet. Figs. 4(a)-(c) compare the near-field (r, t) spatiotemporal intensity profiles in logarithmic intensity scale, so as to better visualize the entire spatiotemporal structure of the light bullet. Figures 4(d)-(f) present the corresponding angularly resolved (θ, λ) spectra, as measured by scanning the far-field (at 25 cm distance from the exit face of sapphire sample) with a $200\text{-}\mu\text{m}$ fiber tip of a fiber spectrometer (AvaSpec-NIR256-2.5, Avantes). The angularly resolved spectra suggest the occurrence of an elliptical, or O-shaped, pattern of conical emission, that is expected from Kerr-driven spatiotemporal instability gain profile in the case of anomalous GVD [37, 38].

The near and far field intensity profiles are combined together to obtain the full spatio-temporal phase profile of the light bullets by means of an iterative Gerchberg-Saxton retrieval algorithm, see [39] for details. The gradient of the retrieved phase profile is used to explicitly visualize the transverse energy density flux in the full spatial and temporal coordinates, as shown normalized in Figs. 4(g), (h) and (i), along with overlaid contour plot of the retrieved intensity profiles. Here the color coding is the same as in [40], where blue and red colors indicate downward and upward fluxes with respect to the vertical axis, respectively.

The transverse energy density flux of the light bullet [Fig. 4(h), (i)] indicates a radially symmetric pulse front tilt resulting from strong space-time coupling, and

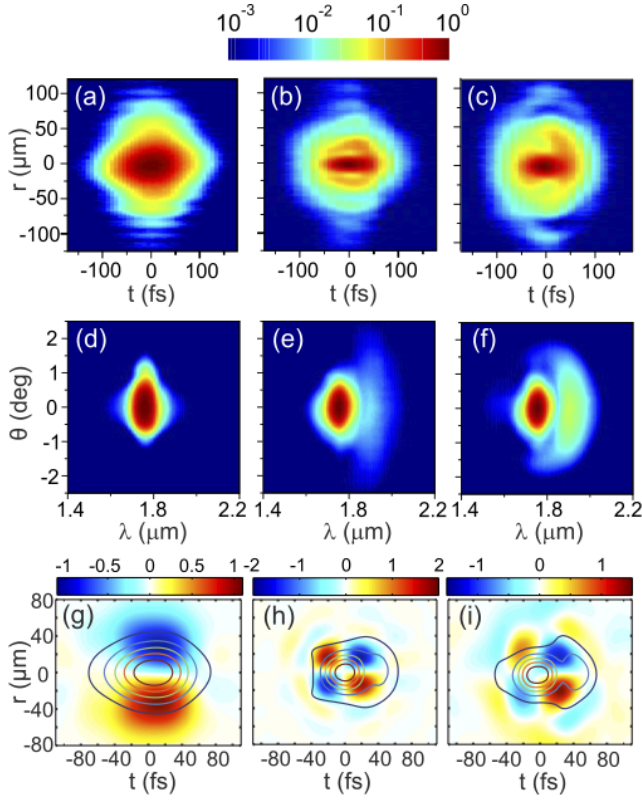


FIG. 4: (Color online) Spatiotemporal intensity profiles (shown in logarithmic intensity scale) of (a) the input wave packet, and the light bullet at (b) $z = 6.0$ mm, (c) $z = 9.0$ mm. (d), (e) and (f) show the corresponding angularly resolved spectra. (g), (h) and (i) show the corresponding retrieved transverse energy fluxes, see text for details.

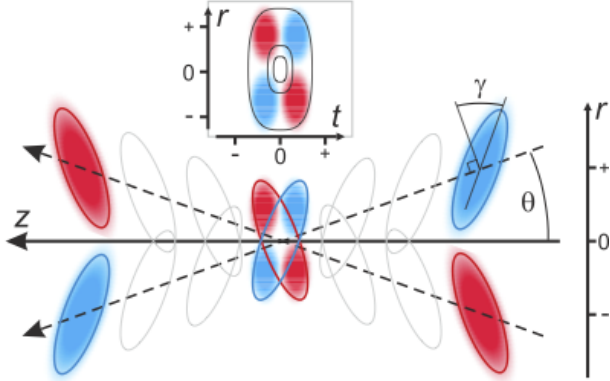


FIG. 5: (Color online) Schematic representation of transverse energy flux in ultrashort-pulsed (polychromatic) Bessel beam with subliminally propagating envelope peak. θ and γ are arbitrary cone and pulse-front tilt angles, respectively.

the spatiotemporal distribution of the currents is almost identical to that of a stationary, polychromatic Bessel beam with subliminally propagating envelope peak [40], as schematically depicted in Fig. 5. The established subluminal propagation of the envelope peak is very much

in line with the results of numerical simulations in fused silica [31, 41], where the position of the peak is shown to continuously shift toward positive times with propagation. The radially symmetric pulse-front tilt, which owes to angular dispersion [42], explains the observed features of temporal behavior of the light bullet in the nonlinear and linear (free space) propagation regimes, as illustrated Fig. 2(b). The propagation angles of the spectral components comprising the light bullet compensate for material dispersion in dispersive medium, whereas such angular distribution causes the dispersive spreading of the pulse, as the bullet exits the dispersive medium and propagates in free space. In addition, presence of the pulse-front tilt may readily explain the reported pulsewidth dependence on the aperture size in the autocorrelation measurements [30]. We underline that a soliton or soliton-like wavepacket would be expected to exhibit a flat phase and hence no transverse energy density flow in the spatiotemporal domain. Conversely, the conical flux unveiled here is inherent to polychromatic Bessel-like pulses and hence serves as unambiguous demonstration of the nature of the light bullets generated by self-focusing in a bulk dielectric media with anomalous GVD. More precisely, the entirety of established properties of the bullet: quasistationary O-shaped spatiotemporal intensity profile and characteristic angularly-resolved spectrum, Bessel-like spatial intensity distribution and transverse energy flux along with nonlinear and linear (free-space) propagation features closely resemble those of the nonlinear O-waves featuring weak losses and subliminally propagating envelope peak [32].

In conclusion, we uncovered the nature of three-dimensional light bullets generated from self-focusing of intense femtosecond pulses in bulk dielectric media with anomalous GVD. Self-focusing dynamics of 100 fs pulses at center wavelength of $1.8 \mu\text{m}$ in sapphire was experimentally captured in detail in full four-dimensional (x, y, z, t) space by means of three-dimensional imaging technique. We demonstrate that the emerging three-dimensional light bullets consist of a sharply localized high-intensity core, which carries the self-compressed pulse and a weak, delocalized low-intensity periphery, comprising a Bessel-like beam. We explicitly demonstrate that the seemingly weak periphery as viewed in linear intensity scale, is nonetheless an important integral part of the overall wave packet, as it continuously balances energy losses in the central core and prevents it from spreading during its linear and nonlinear propagation. We disclose that spatiotemporal reshaping of the input Gaussian wave packet results in development of a very distinct spatiotemporal flow of the energy that is not compatible with a spatiotemporal soliton, but rather finds a natural explanation in terms of a polychromatic Bessel beam, which could be qualified as a nonlinear O-wave which has weak losses and subliminally propagating envelope peak [32]. As a consequence of this, the light bullets exhibit a rather remarkable behavior as they exit

the sample and propagate in free space (air), i.e. in the absence of any nonlinear or dispersive effects: the bullets disperse temporally, yet continue to propagate with strongly suppressed diffraction. We expect that these important features are characteristic to an entire family of spatiotemporal light bullets, which are generated by femtosecond filamentation in bulk dielectric media with anomalous GVD and should be carefully accounted for building the basis for diverse future applications that may require a simple setup for creating intense, temporally compressed and sub-diffractive wave packets [43].

This research was funded by the European Social Fund under the Global Grant measure, grant No. VP1-3.1-ŠMM-07-K-03-001. D.F. acknowledges financial support from the European Research Council under the European Unions Seventh Framework Programme (FP/2007-2013)/ERC GA 306559.

-
- [1] F. Wise and P. Di Trapani, *Opt. Photon. News* **13**(2), 28 (2002).
 - [2] B. A. Malomed, D. Mihalache, F. Wise, and L. Torner, *J. Opt. B* **7**, R53 (2005).
 - [3] D. Mihalache, *Rom. J. Phys.* **57**, 352 (2012).
 - [4] H. Leblond and D. Mihalache, *Phys. Rep.* **523**, 61 (2013).
 - [5] Y. Silberberg, *Opt. Lett.* **15**, 1282 (1990).
 - [6] K. D. Moll, A. L. Gaeta, and G. Fibich, *Phys. Rev. Lett.* **90**, 203902 (2003).
 - [7] M. A. Porras, A. Parola, D. Faccio, A. Couairon, and P. Di Trapani, *Phys. Rev. A* **76**, 011803(R) (2007).
 - [8] M. Belić, N. Petrović, W.-P. Zhong, R.-H. Xie, and G. Chen, *Phys. Rev. Lett.* **101**, 123904 (2008).
 - [9] I. B. Burgess, M. Peccianti, G. Assanto, and R. Morandotti, *Phys. Rev. Lett.* **102**, 203903 (2009).
 - [10] S. Chen and J. M. Dudley, *Phys. Rev. Lett.* **102**, 233903 (2009).
 - [11] L. Torner and Y. V. Kartashov, *Opt. Lett.* **34**, 1129 (2009).
 - [12] V. E. Lobanov, Y. V. Kartashov, and L. Torner, *Phys. Rev. Lett.* **105**, 033901 (2010).
 - [13] S. Minardi, F. Eilenberger, Y. V. Kartashov, A. Szameit, U. Röpke, J. Kobelke, K. Schuster, H. Bartelt, S. Nolte, L. Torner, F. Lederer, A. Tünnermann, and T. Pertsch, *Phys. Rev. Lett.* **105**, 263901 (2010).
 - [14] P. Saari and K. Reivelt, *Phys. Rev. Lett.* **79**, 4135 (1997).
 - [15] A. Chong, W. H. Renninger, D. N. Christodoulides, and F. W. Wise, *Nature Photon.* **4**, 103 (2010).
 - [16] D. Abdollahpour, S. Suntsov, D. G. Papazoglou, and S. Tzortzakis, *Phys. Rev. Lett.* **105**, 253901 (2010).
 - [17] M. Bock, S. K. Das, and R. Grunwald, *Opt. Express* **20**, 12563 (2012).
 - [18] C. Conti, S. Trillo, P. Di Trapani, G. Valiulis, A. Piskarskas, O. Jedrkiewicz, and J. Trull, *Phys. Rev. Lett.* **90**, 170406 (2003).
 - [19] P. Di Trapani, G. Valiulis, A. Piskarskas, O. Jedrkiewicz, J. Trull, C. Conti, and S. Trillo, *Phys. Rev. Lett.* **91**, 093904 (2003).
 - [20] P. Panagiotopoulos, D. G. Papazoglou, A. Couairon, and S. Tzortzakis, *Nature Commun.* **4**, 2622 (2013).
 - [21] M. Kolesik, E. M. Wright, and J. V. Moloney, *Phys. Rev. Lett.* **92**, 253901 (2004).
 - [22] A. Couairon, E. Gaižauskas, D. Faccio, A. Dubietis, and P. Di Trapani, *Phys. Rev. E* **73**, 016608 (2006).
 - [23] D. Faccio, M. A. Porras, A. Dubietis, F. Bragheri, A. Couairon, and P. Di Trapani, *Phys. Rev. Lett.* **96**, 193901 (2006).
 - [24] A. Couairon and A. Mysyrowicz, *Phys. Rep.* **441**, 47 (2007).
 - [25] K. D. Moll and A. Gaeta, *Opt. Lett.* **29**, 995 (2004).
 - [26] L. Bergé and S. Skupin, *Phys. Rev. E* **71**, 065601R (2005).
 - [27] J. Liu, R. Li, and Z. Xu, *Phys. Rev. A* **74**, 043801 (2006).
 - [28] S. Skupin, and L. Bergé, *Physica D* **220**, 14 (2006).
 - [29] S. V. Chekalin, V. O. Kompanets, E. O. Smetanina, and V. P. Kandidov, *Quantum Electron.* **43**, 3261 (2013).
 - [30] E. O. Smetanina, V. O. Kompanets, A. E. Dormidonov, S. V. Chekalin, and V. P. Kandidov, *Laser Phys. Lett.* **10**, 105401 (2013).
 - [31] M. Durand, A. Jarnac, A. Houard, Y. Liu, S. Grabielle, N. Forget, A. Durécu, A. Couairon, and A. Mysyrowicz, *Phys. Rev. Lett.* **110**, 115003 (2013).
 - [32] M. A. Porras, A. Parola, and P. Di Trapani, *J. Opt. Soc. Am. B* **22**, 1406 (2005).
 - [33] D. Majus, V. Jukna, G. Tamošauskas, G. Valiulis, and A. Dubietis, *Phys. Rev. A* **81**, 043811 (2010).
 - [34] D. Faccio, M. Clerici, A. Averchi, A. Lotti, O. Jedrkiewicz, A. Dubietis, G. Tamošauskas, A. Couairon, F. Bragheri, D. Papazoglou, S. Tzortzakis, and P. Di Trapani, *Phys. Rev. A* **78**, 033826 (2008).
 - [35] A. Dubietis, E. Gaižauskas, G. Tamošauskas, and P. Di Trapani, *Phys. Rev. Lett.* **92**, 253903 (2004).
 - [36] A. Dubietis, E. Kučinskas, G. Tamošauskas, E. Gaižauskas, M. A. Porras, and P. Di Trapani, *Opt. Lett.* **29**, 2893 (2004).
 - [37] M. A. Porras, A. Dubietis, E. Kučinskas, F. Bragheri, V. Degiorgio, A. Couairon, D. Faccio, and P. Di Trapani, *Opt. Lett.* **30**, 3398 (2005).
 - [38] M. A. Porras, A. Dubietis, A. Matijosius, R. Piskarskas, F. Bragheri, A. Averchi, and P. Di Trapani, *J. Opt. Soc. Am. B* **24**, 581 (2007).
 - [39] D. Faccio, A. Lotti, A. Matijosius, F. Bragheri, V. Degiorgio, A. Couairon, and P. Di Trapani, *Opt. Express* **17**, 8193 (2009).
 - [40] A. Lotti, A. Couairon, D. Faccio, and P. Di Trapani, *Phys. Rev. A* **81**, 023810 (2010).
 - [41] M. Durand, K. Lim, V. Jukna, E. McKee, M. Baudelet, A. Houard, M. Richardson, A. Mysyrowicz, and A. Couairon, *Phys. Rev. A* **87**, 043820 (2013).
 - [42] M. A. Porras, G. Valiulis, and P. Di Trapani, *Phys. Rev. E* **68**, 016613 (2003).
 - [43] M. Hemmer, M. Baudisch, A. Thai, A. Couairon, and J. Biegert, *Opt. Express* **21**, 28095 (2013).